

Aperture size effects on backscatter intensity measurements in Earth and space remote sensing

Mikko Kaasalainen¹ and Sanna Kaasalainen^{2,*}

¹*Department of Mathematics and Statistics, P.O. Box 68 (Gustaf Hällströöminkatu 2b),
00014 University of Helsinki, Finland*

²*Department of Remote Sensing and Photogrammetry, Finnish Geodetic Institute, Geodeetinrinne 2,
P.O. Box 15, 02431 Masala, Finland*

*Corresponding author: Sanna.Kaasalainen@fgi.fi

Received October 16, 2007; revised February 1, 2008; accepted March 10, 2008;
posted March 19, 2008 (Doc. ID 88690); published April 24, 2008

Most materials show a peaked intensity versus phase (light-source–target–detector angle) curve. For nonnegligible angular apertures of the source and/or the detector, the measured intensity at and near zero phase (backscatter) is lower than the real one. We derive an averaging aperture integral that represents this effect, and with it we invert measured intensity values to obtain the actual intensity curve. We also give a practical formula for estimating the magnitude of the aperture effect in zero-phase intensity measurements and show that only two such measurements made at different apertures are sufficient for deriving the real intensity. These corrections are needed in the comparison of measured reflectances in an increasing number of validation efforts for remote sensing applications requiring ground truth measurements. © 2008 Optical Society of America

OCIS codes: 140.0140, 280.1350, 290.1350.

1. INTRODUCTION

There are several applications in Earth and space sciences that deal with the measurement of backscattered intensity signal. These fields include both active and passive remote sensing from laser scanners [1–3] and radars (e.g., [4]) to airborne passive sensors operating close to backscatter [5]. Backscatter is also investigated in planetary and space science in connection with telescopic or laboratory research of planetary regoliths and their analogs [6–8] or spaceborne Earth-observing satellites, such as NASA's ICESat, where a spaceborne lidar is implemented [9], as well as in physical scattering studies [10,11].

The peculiar characteristics of light intensity at the backscatter geometry set some major challenges to the accurate radiometric calibration of the intensity signal, especially in terrestrial applications and laboratory reference studies that aim at the validation of air or spaceborne results [4,12,13], or in a wide range of other laboratory implications of backscatter measurement [10,14,15]. There are physical studies on backscatter effects in the remote sensing context [16], but the physical nature of all these effects is not yet fully understood. In practice, the nonlinear surge in target brightness toward the exact backscatter needs to be calibrated so that the reflectances measured at backscatter can be compared with those acquired by integrating instruments or those operating at other directions [17]. This requires knowledge of the characteristic backscatter properties of the target and an accurate description of the instrument dimensions, which also have a strong effect on backscatter measurements.

As discussed in [18], the aperture widths of the light

source and detector typically cause a significant flattening of the measured intensity versus phase curve at phase (source–sample–detector) angles below $\theta_0 = (\alpha_1 + \alpha_2)/2$, where α_1 and α_2 are, respectively, the angular aperture widths of the source and the detector as seen from the sample (see Fig. 1). Here we rigorously define this aperture effect and investigate its role in the reconstruction of the intensity profile and the comparison of zero-phase (often referred to as “exact backscatter”) intensity measurements made at different apertures.

The recent increase in terrestrial laser scanners in remote sensing applications [19], together with the growing demand for laser-scanner-based reflectance measurement and calibration [13,20–22], has made the repeatability of reflectance measurement an important issue. This is particularly important in applications where ground truth data for airborne sensors are collected by terrestrial laser scanners [13] or other backscatter instruments, such as radars [4]. This emphasizes the question of aperture sizes and their effect on the angular resolution of backscatter measurement. The typical aperture size of an airborne laser scanner varies from 8 to 15 cm [23], which means that the maximum combined source and detector aperture angle is about 0.03° at low (e.g., 500 m) flight altitudes. As the distances in terrestrial and laboratory applications are much smaller and the aperture sizes in, e.g., terrestrial laser scanners are of the order of a few centimeters, the aperture angles are significantly larger. The laser beam widths in these applications typically vary in the millimeter scale, which alone increases the combined aperture width at close distances (e.g., a 3 mm laser exit beam width at a distance of 1 m from the sample causes a 0.2° increase). This results in different reflectance signals

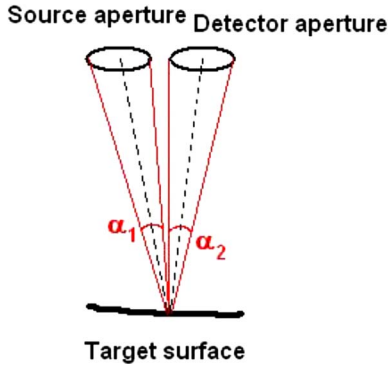


Fig. 1. (Color online) Aperture and phase angle geometry of an intensity measurement.

from the same target and complicates the comparison of data between different instruments.

Since the calibration and usage of laser scanner intensity are at a very preliminary state of study in the field of laser scanning, the impact of errors in the generation of surface models and target classification has to be assessed in future studies. Preliminary results from airborne and terrestrial laser scanning campaigns suggest that, for the current detectors optimized for range rather than intensity measurements, random instrumental errors may play the strongest role [13]. However, aperture size effects are a source of systematic errors that can readily be corrected for, as we will show below.

This paper presents a description of the aperture size effects on the backscattered intensity and provides a practical method for estimating and correcting the intensity effects caused by an increased angular aperture width in terrestrial and laboratory applications of backscatter measurement. We define the size effects in Section 2 and examine the inverse problem of reconstructing the correct intensity in Section 3. In Section 4 we present useful approximate formulas for estimating the correct backscatter intensity in measurement calibration and show that our formulation is quite consistent with experimental data. We present our conclusions and discuss the role of aperture size effects in Section 5.

2. APERTURE INTEGRALS

Let us denote the theoretical phase-angle (θ) dependent intensity of the light scattered from the sample by $I(\theta)$ (assuming fixed source–sample–detector distance and source intensity). Due to the nonzero apertures of the source and the detector, this intensity cannot be observed directly. The observed intensity $I_o(\theta)$ is an averaging of $I(\theta)$ produced by light rays scattered at various phase angles between $\theta - \theta_0$ and $\theta + \theta_0$ (see Fig. 1; we assume the apertures to be perpendicular to the direction to the target).

Let us define the aperture integral $I_A[\theta; \alpha; I(\theta)]$ as the integral for observed intensity with one zero-size aperture (source or detector) and one aperture of angular width α , obtained by averaging the intensity integrated over the aperture. Denoting polar coordinates (with the center of the aperture for the origin) by (ρ, ϕ) , we have

$$I_A[\theta; \alpha; I(\theta)] = \frac{8\pi}{\alpha^2} \int_0^\pi \int_0^{\alpha/2} I(\sqrt{\theta^2 + 2\theta\rho \cos \phi + \rho^2}) \rho d\rho d\phi. \quad (1)$$

Allowing the other aperture to have a nonvanishing size β yields the double-aperture integral I_{A^2} , which is the quadruple integral

$$I_{A^2}[\theta; \alpha, \beta; I(\theta)] = I_A[\theta; \beta; I_A[\theta; \alpha; I(\theta)]]. \quad (2)$$

This is symmetric with respect to the apertures: $I_{A^2}(\alpha, \beta) \equiv I_{A^2}(\beta, \alpha) = I_o$. Here we neglect further weight functions (e.g., due to the light source) inside the aperture(s) in the integral as well as third-order effects (integration of I_{A^2} over the laser spot on the sample, the effect of which vanishes at $\theta=0$ in any case), as their contribution to the already small total effect is minor in practice.

Both I_A and I_{A^2} are straightforward and fast to evaluate numerically (it is convenient to interpolate between suitable previously computed single-aperture values of I_A when computing the double-aperture integral I_{A^2}). By numerical comparisons, we have found that the simple slit integral of [18], a one-dimensional intensity integral over a slit of given width α , often turns out to be a good approximation of $I_{A^2}(\beta, \gamma)$ when $\alpha = \beta + \gamma$ and $\beta \approx \gamma$ [but not of $I_A(\alpha)$, which gives more weight to the edges of the aperture and thus produces a more flattening effect than the one-dimensional integral]. This is useful for practical approximations, as we will show below.

3. INVERSE PROBLEM

Assuming a suitable functional representation for $I(\theta)$, one can determine the observed intensities by solving the inverse problem of determining the values of the function model parameters \mathbf{P} such that the resulting I_o from Eq. (2) best fits the N observed intensities $I_i^{(\text{obs})}$ at phase angles θ_i . This can be formulated as least-squares (χ^2) minimization:

$$\chi^2 = \sum_{i=1}^N (I_i^{(\text{obs})} - I_{A^2}[\theta_i; \alpha, \beta; I(\theta; \mathbf{P})])^2, \quad (3)$$

where the argument $I(\theta; \mathbf{P})$ denotes the functional form of I given the parameters \mathbf{P} .

In principle, I could be represented as a function series with linear coefficients (e.g., a simple polynomial series), resulting in a simple linear parameter fit. With a well-sampled near-zero phase region, this may be sufficient for analyzing the difference $I(\theta) - I_o(\theta)$ at $\theta \approx 0$, even though with larger θ , this usually results in nonmonotonic (i.e., physically unrealistic) and not sufficiently smooth $I(\theta)$. Another possibility is to use models designed to represent typical phase-angle behavior, such as the exponential-linear one used in [18,24]:

$$I(\theta) = c \exp(-\theta/\omega) + k\theta + d, \quad (4)$$

where $\mathbf{P} = (c, \omega, k, d)$ are free parameters. In Fig. 2 we show an example of solving for these parameters with nonlinear optimization as in [24]. The data are from a reindeer lichen [*Cladina stellaris* (Opiz) Brodo] sample, measured with 0.3° aperture for the detector and 0.2° for

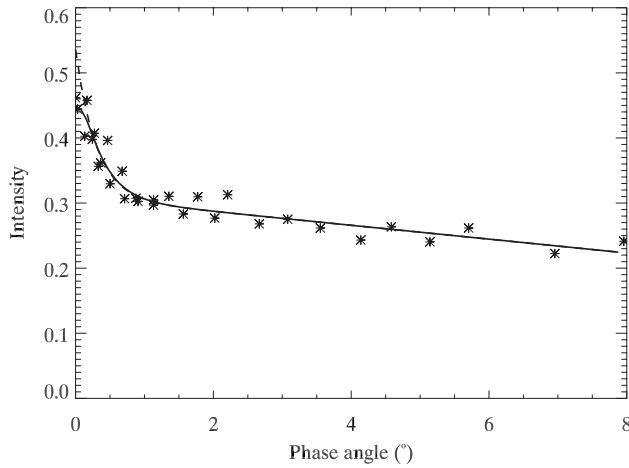


Fig. 2. Intensity measurements of reindeer lichen [25] (asterisks) with modeled I_o (solid curve) and estimated I (dashed curve).

the laser (see [25] for more details). As can be seen from Fig. 2, the obtained intensity function parameters $c = 0.31$, $\omega = 0.3^\circ$, $k = -0.02$, $d = 0.23$ reproduce the observed points well and show that the actual intensity peak at zero phase is almost 20% higher than the observed value.

The assumed form (4) is more restrictive than a general function series, but this also serves a regularizing purpose: On experimenting with a polynomial series, we found that the estimate of the peak intensity $I(0)$ fluctuates considerably, depending on the chosen maximum order and the noise level of the data. The form (4) may give a slightly conservative estimate of $I(0)$, as it is not well suited for representing extreme zero-phase surges, but it is also more stable in inversion. A spiky $\theta \rightarrow 0$ part of $I(\theta)$, much narrower than the aperture resolution, contributes relatively little to the smoothed I_{A^2} , so the top $I(0)$ level, unless regularized, is indeed prone to instability. In typical laboratory measurements, the relative surge magnitude should be at least some 15% of the measured zero-phase intensity $I_o(0)$ for the corrected $I(0)$ to stand above the noise level of I_o near zero phase [cf. Fig. 2 and 4 (below)].

4. RESOLUTION EFFECT IN MEASUREMENT CALIBRATION

Using the slit approximation of [18], i.e., integrating Eq. (4) over a width of α , and setting $\theta = 0$, we obtain a rough estimate for the zero-phase intensity decrease as a function of the aperture resolution and the steepness and amplitude of the zero-phase surge:

$$\frac{I_o(0)}{I(0)} = \frac{1}{c+d} \left[\frac{2\omega}{\alpha} c \left[1 - \exp\left(-\frac{\alpha}{2\omega}\right) \right] + k\alpha/4 + d \right], \quad (5)$$

where I is assumed to be of the exponential-linear form (4). The slit width is given by $\alpha = \alpha_1 + \alpha_2$, and we assume $\alpha_1 \approx \alpha_2$. For realistic values of k , the contribution of the k term is negligible for the value of Eq. (5), so we can write Eq. (5) as

$$\frac{I_o(0)}{I(0)} \approx 1 - f\left(\frac{\alpha}{2\omega}\right) \frac{c}{c+d}, \quad (6)$$

where

$$f(x) = \frac{x}{2!} - \frac{x^2}{3!} + \dots \quad (7)$$

This gives an approximate value of the expected intensity error due to averaging. When the summed apertures are smaller than the scale width ω of the zero-phase surge ($\alpha/2\omega \ll 1$), the relative decrease D in measured intensity is thus approximately

$$D = 1 - \frac{I_o(0)}{I(0)} \approx \frac{s\alpha}{4\omega}, \quad (8)$$

where $s = c/(c+d)$ describes the relative amplitude of the surge. This is a useful formula for a rough estimate of D for peaked intensity curves, as the amplitude and the width of the peak can be understood in a general sense.

Due to the linearity of Eq. (8), one can estimate the surge amplitude/peak scale width ratio s/ω and the real zero intensity from just two different I_o measurements I_i and I_j made at apertures α_i and α_j :

$$\frac{s}{\omega} = 4 \frac{I_i/I_j - 1}{(I_i/I_j)\alpha_j - \alpha_i}, \quad (9)$$

and

$$I(0) = \frac{I_i\alpha_j - I_j\alpha_i}{\alpha_j - \alpha_i}. \quad (10)$$

Here one should note that the error of $I(0)$ scales as $\Delta I(0) = (\alpha_i + \alpha_j)\Delta I/|\alpha_i - \alpha_j|$, where ΔI describes the error of the intensity measurements. One α should thus be as small as possible and the other one as large as feasible within the $\alpha < 2\omega$ regime. In any case, such pairwise estimates require accurate measurements due to the amplifying scaling of errors, and there is always the danger of inadvertent use of outliers, leading to meaningless results. The measurements should be repeated at least a few times to establish an average estimate.

In Table 1, we show measured $I_o(0)$ values for a PVC-coated polyester tarp of 70% diffuse intensity, which has been manufactured and used as a calibration target in airborne imagery and laser scanning. The instrument is described in Fig. 3 (with more details in [13]). The measurements were obtained with varying detector apertures

Table 1. Peak Intensity Decrease D due to Growing Aperture

Aperture ($^\circ$)	$I_o(0)^a$	Estimated $I(0)$	D from I_{A^2}	D from (8)	$I(0)_{1i}$
0.52	0.845	0.92	0.08	0.09	—
0.62	0.829	0.92	0.10	0.10	0.93
0.81	0.809	0.92	0.12	0.15	0.91
1.01	0.770	0.91	0.15	0.17	0.92
1.34	0.732	0.90	0.19	0.22	0.92
1.78	0.720	0.92	0.22	0.30	0.90

^a $I_o(0)$ denotes the measured intensity at backscatter. $I(0)$ is the aperture-corrected estimate for the true $I(0)$. $I(0)_{1i}$ is the pairwise approximation from Eq. (10).

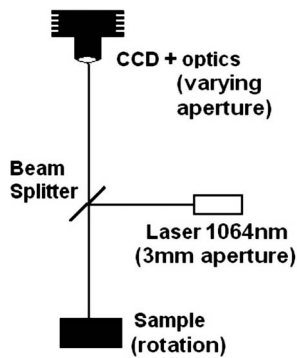


Fig. 3. Laboratory measurement for $I_o(0)$ at various detector apertures. The distances from the sample surface to the laser and to the detector were 82 cm and 108 cm, respectively. The detector (camera objective) f -number was changed to obtain different aperture angles, shown in Table 1.

and a fixed laser aperture 0.24° (combined angular aperture α is shown). The $I_o(0)$ intensities were calibrated with a 99% Spectralon reference plate measured similarly to the target. We also show the estimated $I(0)$ from the I_{A^2} model for each aperture and D from both I_{A^2} and approximation (8). The exponential-linear model for $I(\theta)$ was determined as above using the measured phase-intensity measurement for this material, shown in Fig. 4. Note that the intensity scales are different in Table 1 and Fig. 4 due to different measurements, so the absolute intensity for $I(0)$ must be determined separately for each aperture. All these values are close to 0.92, and their variation is consistent with the noise level of the measurements, so we conclude that the I_{A^2} model reproduces the aperture effect well. Including minor details in the model would make it less practicable, and in the inverse problem their effect would be eclipsed by the model uncertainty of $I(\theta)$. Approximation (8) yields $D \approx 0.17\alpha$ [deg]. This value holds rather well even after the $\alpha < 2\omega$ regime (i.e., here $\alpha < 1^\circ$).

We also show the estimated $I(0)_{1i}$ from Eq. (10) for each 1, i pair. This value is surprisingly stable (the error level of the aperture-change measurement is lower than that of geometry-changing setups) and close to the one computed from I_{A^2} . Note that it is not based on any model parameters or any other *a priori* assumptions of the surface

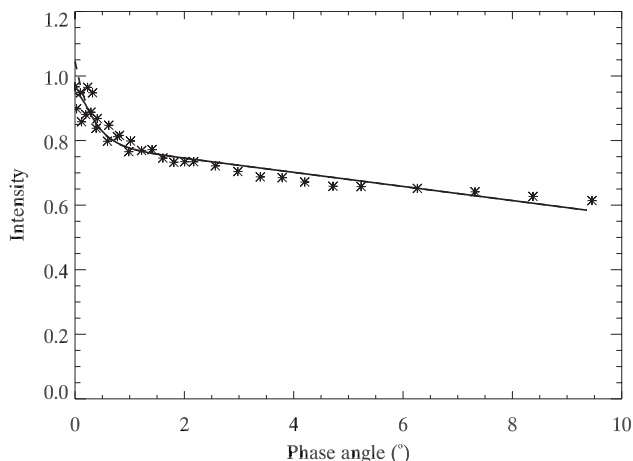


Fig. 4. Intensity measurements (asterisks) of the sample with modeled I_o (solid curve) and estimated I (dashed curve).

characteristics. The only assumption needed for deriving $I(0)$ in Eq. (10) is that D be linear in α . The related pairwise s/ω values from Eq. (9) vary more but yield a good average estimate of the ratio of the surge characteristics without a full intensity curve measurement.

5. DISCUSSION

We have shown that the instrument aperture size plays a significant role in the backscatter intensity measurement. This must be taken into account in remote sensing ground truth experiments carried out with nonnegligible instrumental aperture widths. We provide a simple formula for estimating the decrease in the measured intensity depending on the aperture size and the backscattering properties of the target surface [see Eq. (8)]. We also provide a formula [see Eq. (10)] for approximating the actual intensity value at exact backscatter, based on only two separate measurements with different aperture sizes and requiring no other information about the surface.

The range differences between airborne and terrestrial laser scanning provide a practical example of the use of Eq. (8) in the validation of remote sensing and ground truth experiments. Asphalts, gravels, and sands represent typical remote sensing land targets, with backscatter peak enhancement toward 0° typically varying between 20% and 50% [17]. Assuming a 30% peak amplitude and 0.5° width, the corresponding decrease in backscatter intensity according to Eq. (8) is 1.5% for each 0.1° in combined aperture angle. For a typical terrestrial laser scanner measuring at 2 m distance, the combined aperture angle with a 3 mm laser beam width and a 5 cm detector aperture is 1.5° , which results in over 20% drop in the target intensity. The corresponding drop in intensity for an airborne laser scanner measuring the same target surface at, say, 0.03° aperture is only 0.5%, which means that there is about 20% difference in calibrated intensities caused by the differences in the angular aperture size alone. The correction with Eq. (10) is possible, given that a reflectance calibration method (e.g., with calibration targets and the atmospheric corrections for the long-range measurement) is available. As the standard errors in reflectance measured with current airborne laser scanners are typically of order 5% [26], the impact of aperture size effects is small in airborne applications, but it must be taken into account when comparing the airborne laser reflectances with, e.g., terrestrial laser measurements obtained with significantly larger apertures.

In planetary science, phase angles very close to zero are often obtained in both ground-based photometry and space probe missions. Due to the distances, the angular aperture of the detector is negligible, but the apparent diameter of the Sun is usually at least a few tenths of a degree. The flattening of the observed intensity curve is now given by the aperture integral $I_A(\theta)$. Depending on the surface material's opposition surge, the apparent zero-phase intensity can thus be a few percent lower than the actual one.

ACKNOWLEDGMENTS

This study was financially supported by the Academy of Finland (projects Improving the Applicability of Intensity

Information in Laser Scanning and New Mathematical Methods in Planetary and Galactic Research).

REFERENCES

1. W. Wagner, A. Ullrich, V. Ducic, T. Melzer, and N. Studnicka, "Gaussian decomposition and calibration of a novel small-footprint full-waveform digitising airborne laser scanner," *ISPRS J. Photogramm. Remote Sens.* **60**, 100–112 (2006).
2. S. Kaasalainen, J. Hyypä, P. Litkey, H. Hyypä, E. Ahokas, A. Kukko, and H. Kaartinen, "Radiometric calibration of als intensity," in *Proceedings of the ISPRS Workshop on Laser Scanning 2007 and SilviLaser 2007*, International Archives of Photogrammetry, Remote Sensing and Spatial Information Sciences (International Society for Photogrammetry and Remote Sensing, 2007), Vol. XXXVI (Part 3/W52), pp. 201–205. CD-ROM. <http://www.isprs.org>.
3. D. N. M. Donoghue, P. J. Watt, N. J. Cox, and J. Wilson, "Remote sensing of species mixtures in conifer plantations using lidar height and intensity data," *Remote Sens. Environ.* **110**, 509–522 (2007).
4. K. K. Williams and R. Greeley, "Laboratory and field measurements of the modification of radar backscatter by sand," *Remote Sens. Environ.* **89**, 29–40 (2004).
5. F. C. de Coca, F. M. Bron, M. Leroy, and F. J. Garcia-Haro, "Airborne measurement of hot spot reflectance signatures," *Remote Sens. Environ.* **90**, 63–75 (2004).
6. A. J. Verbiscer, R. G. French, and C. A. McGhee, "The opposition surge of enceladus: Hst observations 3381022 nm," *Icarus* **173**, 66–83 (2005).
7. J. L. Piatek, B. W. Hapke, R. M. Nelson, W. D. Smythe, and A. S. Hale, "Scattering properties of planetary regolith analogs," *Icarus* **34**, 531–545 (2004).
8. S. Bondarenko, A. Ovcharenko, Y. Shkuratov, G. Videen, J. Eversole, and M. Hart, "Light backscatter by surfaces composed of small spherical particles," *Appl. Opt.* **45**, 3871–3877 (2006).
9. D. J. Harding and C. C. Carabajal, "ICESat waveform measurements of within-footprint topographic relief and vegetation vertical structure," *Geophys. Res. Lett.* **32**, L21S10 (2005). doi: 10.1029/2005GL023471.
10. M.-J. Kim, J. C. Dainty, A. T. Friberg, and A. J. Sant, "Experimental study of enhanced backscattering from one- and two-dimensional random rough surfaces," *J. Opt. Soc. Am. A* **7**, 569–577 (1990).
11. A. Ovcharenko, S. Bondarenko, Y. S. Cathy Scotto, C. Merritt, M. Hart, J. Eversole, and G. Videen, "Backscatter effects of surfaces composed of dry biological particles," *J. Quant. Spectrosc. Radiat. Transf.* **101**, 462–470 (2006).
12. J. Ellis, P. Caillard, and A. Dogariu, "Off-diagonal Mueller matrix elements in backscattering from highly diffusive media," *J. Opt. Soc. Am. A* **19**, 43–48 (2002).
13. S. Kaasalainen, A. Kukko, T. Lindroos, P. Litkey, H. Kaartinen, J. Hyypä, and E. Ahokas, "Brightness measurements and calibration with airborne and terrestrial laser scanners," *IEEE Trans. Geosci. Remote Sens.* **46**, 528–534 (2008).
14. Y. L. Kim, Y. Liu, V. M. Turzhitsky, H. K. Roy, R. K. Wali, and V. Backman, "Coherent backscattering spectroscopy," *Opt. Lett.* **29**, 1906–1908 (2004).
15. Y. L. Kim, Y. Liu, R. K. Wali, H. K. Roy, and V. Backman, "Low-coherent backscattering spectroscopy for tissue characterization," *Appl. Opt.* **44**, 366–377 (2005).
16. B. Hapke, D. D. Mucci, R. Nelson, and W. Smythe, "The cause of the hot spot in vegetation canopies and soils: shadow-hiding versus coherent backscatter," *Remote Sens. Environ.* **58**, 63–68 (1996).
17. S. Kaasalainen, J. Hyypä, and T. Mielonen, "Laboratory calibration of backscattered intensity for laser scanning land targets," in *Proceedings of the ISPRS Workshop on Laser Scanning 2005*, International Archives of Photogrammetry, Remote Sensing and Spatial Information Sciences (International Society for Photogrammetry and Remote Sensing, 2005), Vol. XXXVI (Part 3/W19), pp. 13–17. CD-ROM. <http://www.isprs.org>.
18. S. Kaasalainen, J. Peltoniemi, J. Näränen, J. Suomalainen, M. Kaasalainen, and F. Stenman, "Small-angle goniometry for backscattering measurements in the broadband spectrum," *Appl. Opt.* **44**, 1485–1490 (2005).
19. F. M. Danson, D. Hetherington, F. Morsdorf, B. Koetz, and B. Allgower, "Forest canopy gap fraction from terrestrial laser scanning," *IEEE Geosci. Remote Sens. Lett.* **4**, 157–160 (2007).
20. F. Coren and P. Sterzai, "Radiometric correction in laser scanning," *Int. J. Remote Sens.* **27**, 3097–3104 (2006).
21. D. S. Boyd and R. A. Hill, "Validation of airborne lidar intensity values from a forested landscape using hmap data: preliminary analyses," in *Proceedings of the ISPRS Workshop on Laser Scanning 2007 and SilviLaser 2007*, International Archives of Photogrammetry, Remote Sensing and Spatial Information Sciences (International Society for Photogrammetry and Remote Sensing, 2007), Vol. XXXVI, (Part 3/W52), pp. 71–76. CD-ROM. <http://www.isprs.org>.
22. C. Hopkinson, "The influence of flying altitude, beam divergence, and pulse repetition frequency on laser pulse return intensity and canopy frequency distribution," *Can. J. Remote Sens.* **33**, 312–324 (2007).
23. A. Wehr and U. Lohr, "Airborne laser scanning—an introduction and overview," *ISPRS J. Photogramm. Remote Sensing* **54**, 68–82 (1999).
24. M. Kaasalainen, J. Torppa, and K. Muinonen, "Optimization methods for asteroid lightcurve inversion. ii. the complete inverse problem," *Icarus* **153**, 37–51 (2001).
25. S. Kaasalainen and M. Rautiainen, "Hot spot reflectance signatures of common boreal lichens," *J. Geophys. Res.* **110**, D20102 (2005). doi:10.1029/2005JD005834.
26. E. Ahokas, S. Kaasalainen, J. Hyypä, and J. Suomalainen, "Calibration of the optech altm 3100 laser scanner intensity data using brightness targets," in *ISPRS Commission I Symposium*, International Archives of Photogrammetry, Remote Sensing and Spatial Information Sciences (International Society for Photogrammetry and Remote Sensing, 2006), p. 36(A1). CD-ROM. <http://www.isprs.org>.